Electronic Supplementary Information (ESI)

Metal ion promoted tautomerization and C-N bond cleavage: conversion of catechol to a *p*-benzoquinone derivative

Pinaki Saha,[a] Amit Saha Roy,[a] Thomas Weyhermüller[b] and Prasanta Ghosh*[,a]

[a]Department of Chemistry, R. K. Mission Residential College, Narendrapur, Kolkata-103, India

[b]Max-Planck-Institut für Chemische Energiekonversion, Stiftstrasse 34-36 / D-45470 Mülheim an der Ruhr, Germany

*Correspondence to: ghosh@pghosh.in

Table of Content

Materials

Reagents or analytical grade materials were obtained from the commercial suppliers and used without further purification. Spectroscopic grade solvents were used for spectroscopic and electrochemical measurements**.**

Experimental section

Syntheses

2,5-bis(*p*-tolylamino)-4-*p*-tolyliminobenzoquinone ($Q_{p\text{-NO}}$)

To a solution of catechol (110 mg, 1 mmol) in MeOH (25 ml), *p*-toluidine (321 mg, 3 mmol) and catalytic amount of iodine were added and the resulting solution was heated to reflux for 90 min. The reaction mixture was cooled at 25°C and allowed to evaporate slowly in air. After 2-3 days, dark red crystals of $Q_{p\text{-NO}}$.MeCN separated out, which were filtered and collected. Yield: 281 mg, 69% (with respect to catechol). ESI (positive ion)- MS in CH_3OH; *m/z*: 408.05 ($Q_{p\text{-NO}}^{+}$). ^{1}H NMR ($CDCl_3$, 300 MHz., 300K): δ (ppm) = 8.64 (s, NH), 7.60 (s, NH), 7.21 (m, 3H), 7.08 (d, J=8.1, 3H), 6.96 (d, J=8.1, 3H), 6.87 (d, J=7.8 Hz, 3H), 6.19 (s, 1H), 6.09 (s, 1H), 2.36 (s, 6H), 2.29 (s, 3H). ^{13}C NMR ($CDCl_3$, 300 MHz, 300 K): δ (ppm) = 180.00 (-C=O), 150.01 (-C-NH-), 135.63, 135.16, 130.10, 130.05, 129.71, 123.45, 121.81, 121.13, 96.87, 89.89, 21.04 ($-CH_3$), 20.90 ($-CH_3$). Anal. Calcd. for $C_{27}H_{25}N_3O$ ($Q_{p\text{-NO}}$): C, 79.58; H, 6.18; N, 10.31. Found: C, 79.31; H, 6.02; N, 10.09. IR (KBr, ν_{max}/cm^{-1}): 3313 (s, N-H), 3282 (s, N-H), 1587 (vs, CPh=N-), 1517 (vs),1482 (s), 1343 (s), 1296 (s), 1175 (w), 820 (s), 628 (w), 506 (w).

$[Pd^{II}(Q_{o\text{-NN}})Cl_2]$.EtOH (1.EtOH)

$PdCl_2$ (177 mg, 1 mmol) was digested to $H_2[PdCl_4]$ using few drops of concentrated HCl and to it EtOH (30 ml) and MeCN (30 ml) solvents were added and heated. To this hot solution mixture $Q_{p\text{-NO}}$ (408 mg, 1 mmol) was added and the mixture was heated to reflux for 45 min. The solutions turned dark green, which was cooled to room temperature. After 3-4 days crystalline green compound of **1**.EtOH separated out which was filtered and the residue was dried in air. The single crystals for X-ray diffraction study were collected from this residue. The residue was dried under high vacuum for analytical measurements. Yield: 380 mg, 74% (with respect to palladium). ESI (positive ion)-MS in CH_3OH; *m/z*: 549.91 (**1**-Cl^-). ^{1}HNMR ($CDCl_3$, 300 MHz., 300K): δ (ppm) = 9.50 (s, OH), 8.11 (s, NH), 7.09 (d, 3H), 6.97 (m, 9H), 5.55 (s, 1H), 5.42 (s, 1H), 3.45 (q, J=5.1, 3H), 2.49 (s, 3H), 2.32 (s, 3H), 2.23 (s, 3H), 1.05 (t, J=5.4, 3H). ^{13}C NMR ($CDCl_3$, 300 MHz, 300 K): δ (ppm) = 169.00 (C-OH), 146.71 (-C-NH-), 143.85 (-C=N-), 143.61 (-C=N-), 130.18, 129.78, 129.07, 128.72, 125.22, 124.71, 123.88, 97.79, 90.18, 56.67 (EtOH), 21.22 ($-CH_3$), 20.03 ($-CH_3$), 18.85 (EtOH). Anal. Calcd. for

$C_{27}H_{25}N_3OPdCl_2$ (**1**): C, 55.43; H, 4.31; N, 7.19. Found: C, 55.24; H, 4.11; N, 7.02. IR (KBr, ν_{max}/cm^{-1}): 3434 (w, -OH), 3244 (vs, N-H), 2913 (s), 1586 (s, PhC=N-), 1557 (vs),1502 (s), 1419 (vs), 1274 (vs), 1054 (w), 813 (s), 679 (w), 497 (w).

[$Rh^{III}(PPh_3)$(*p*-toluidine)(MeCN)Cl_3] (2)

To a hot solution of $Q_{p\text{-NO}}$ (204 mg, 0.5 mmol) in a mixture of EtOH (30 mL) and MeCN (30 mL) solvents, anhydrous $RhCl_3$ (105 mg, 0.5 mmol) and PPh_3 (131 mg, 0.5 mmol) were added. The mixture was refluxed for 45 min in argon atmosphere and allowed to cool at room temperature (298 K). Yellowish-orange crystal of **2** separated out. The mixture was filtered and the residue was dried in air. Yield: 261 mg, 54% (with respect to rhodium). ESI (positive ion)- MS in MeCN; *m/z*: 618 ($\mathbf{2}^+$)(-Cl^-). ^{1}H NMR ($CDCl_3$, 300 MHz, 300K): δ (ppm) = 8.91(s, 2H), 7.83 (d, 2H), 7.81(d, 2H), 7.42 (t, 6H),7.31 (d, 2H), 7.29 (d, 2H), 7.28 (d, 2H), 7.12 (t, 3H), 2.35 (t, 3H), 1.59 (t, 3H). ^{13}C NMR ($CDCl_3$, 300 MHz, 300 K): δ (ppm) = 135.87, 135.79, 135.59, 134.82, 132.51, 132.00, 131.90, 130.11, 129.73, 129.48, 129.28, 129.21, 128.76, 127.83, 127.73, 123.89, 118.51, 114.51 (MeCN), 20.11 (-CH_3), 1.62 (MeCN). Anal. Calcd. for $C_{27}H_{27}N_2PRhCl_3$ (**2**): C, 52.33; H, 4.39; N, 4.52; Found: C, 52.24; H, 4.31; N, 4.41; IR (KBr, ν_{max}/cm^{-1}): 3255 (s, N-H), 3210 (w), 3131 (s, N-H)), 3058 (w), 2918(s), 2324 (vw), 1583 (w), 1513 (vs), 1482 (vs), 1426 (vs), 1384 (s), 1099 (vs), 816(w), 744(vs), 693(vs, $\nu_{Ru-P(sym)}$), 525(vs,$\nu_{Ru-P(asym)}$), 511 (vs).

Direct synthesis of 2 with *p*-toluidine

To a hot mixture of EtOH (20 mL) and MeCN (20 mL) solvents, anhydrous $RhCl_3$ (75 mg, 0.36 mmol), PPh_3 (93.5 mg, 0.36 mmol) and *p*-toluidine (39 mg, 0.36 mmol) were added successively. The mixture was refluxed for 45 min under argon and allowed to cool at room temperature (298 K). Yellowish-orange micro crystalline of **2** separated out. The mixture was filtered and the residue was dried in air. Yield: 136 mg, 61% (with respect to rhodium). ESI (positive ion)- MS peak in MeCN, IR and the ^{1}H NMR data in $CDCl_3$ are similar to above.

2,5-bis(*p*-tolylamino)-*p*-benzoquinone ($Q_{p\text{-OO}}$)

The filtrate after separation of complex **2** obtained from the above reaction was collected and evaporated to dryness. The organic mass was extracted with diethyl ether. Column chromatography in basic alumina of this diethyl ether solution was performed. Elution with 1:1 ether and CH_2Cl_2 solvents mixture and evaporation in high vacuum yield the residue of $Q_{p\text{-OO}}$ product which was dried.

Yield: 55 mg, ~35% (with respect to $Q_{p\text{-NO}}$). ESI (positive ion)- MS in MeOH; *m/z*: 317.96, 316.95 ($Q_{p\text{-OO}}^{+}$). ^{1}H NMR ($CDCl_3$, 300 MHz., 300K): δ (ppm) = 8.64 (s, NH), 7.69 (s, NH), 7.18 (d, J= 8.7 Hz, 2H), 7.08 (d, J= 8.1 Hz, 2H), 6.97 (d, J= 8.1 Hz, 2H), 6.87 (d, J=8.1 Hz, 2H), 6.20 (s, 1H), 6.09 (s, 1H), 2.36 (s, 3H), 2.29 (s, 3H). ^{13}C NMR ($CDCl_3$, 300 MHz, 300 K): δ (ppm) = 180.93 (-C=O), 153.45(-C-NH), 140.81, 130.01, 129.87, 129.51, 123.11, 121.09, 120.78, 96.64, 90.06, 23.74 ($-CH_3$), 22.93 ($-CH_3$). Anal. Calcd. For $C_{20}H_{18}N_2O_2$ ($Q_{p\text{-OO}}$): C, 75.45; H, 5.70; N, 8.80; found: C, 75.39; H, 5.64; N, 8.74; IR (KBr, ν_{max}/cm^{-1}): 3252 (s, -NH), 3028 (w), 2922 (s), 1726 (s),1634 (s), 1579 (vs), 1516 (vs), 1342 (w), 1294 (vs),1177 (s), 1073 (w), 809(s).

Physical measurements

Commercially available spectroscopic grade solvents were used for spectroscopic and electrochemical measurements. The carbon and hydrogen contents of the compounds were obtained from a *Perkin-Elmer 2400 series II* elemental analyzer. IR spectra of the samples were measured from 4000 to 400 cm^{-1} with KBr pellets at room temperature on a *Perkin-Elmer* Spectrum RXI Fourier transform IR spectrophotometer. ^{1}H NMR and ^{13}C NMR spectra in $CDCl_3$ and DMSO solvent were carried out on a *Bruker Avance DPX-300 MHz* spectrometer. ESI mass spectra were recorded on a *micromass Q-TOF* mass spectrometer. Electronic absorption spectra in solution at 298 K were recorded on a *Perkin-Elmer Lambda 25* spectrophotometer in the range of 1100-200 nm. The electroanalytical instrument *BASi Epsilon-EC* for cyclic voltammetry experiments in DMSO and MeCN solution containing 0.20 M tetrabutylammonium hexafluorophosphate as the supporting electrolyte was used. The BASi platinum working electrode, platinum auxiliary electrode and Ag/AgCl reference electrode were used for the measurements. The redox potential data are referenced versus a ferrocenium/ferrocene, Fc^{+}/Fc, couple. EPR spectra were recorded on *Magnettech GmbH MiniScope MS400* EPR spectrometer (equipped with temperature controller TC H03), where the microwave frequency was measured with a frequency counter FC400.

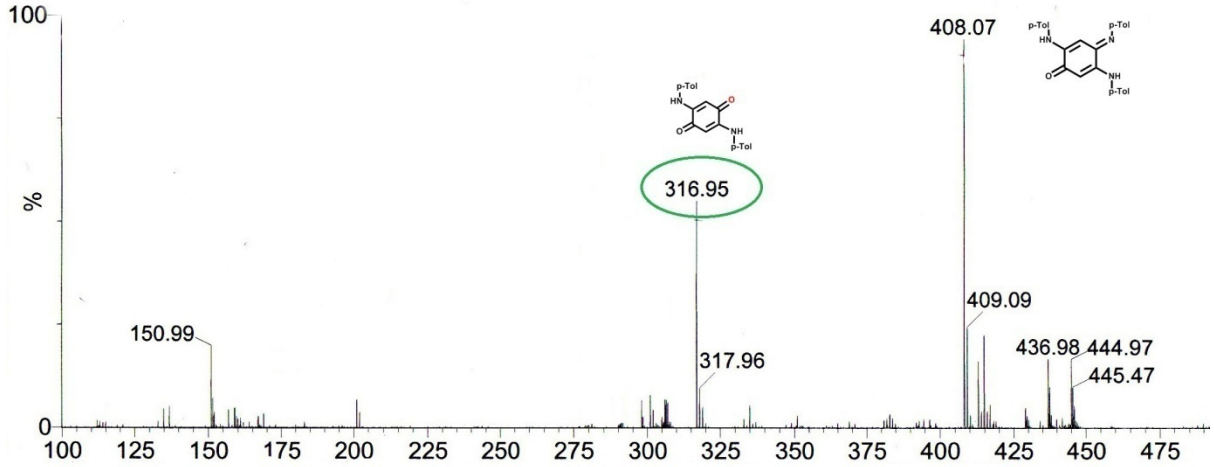

Fig. S1. ESI (positive ion) mass spectrum of $Q_{p\text{-}OO}$ in MeOH solvent.

X-ray crystallographic data collection and refinement of the structures

Single crystals of $Q_{p\text{-}NO}$.MeCN, **1**.EtOH and **2** were picked up with a nylon loop, which were mounted on a Bruker Kappa CCD diffractometer equipped with a molybdenum target rotating-anode X-ray source and a graphite monochromator (Mo Kα, λ = 0.71073 Å). Final cell constants were obtained from least-squares fits of all measured reflections. Structures were readily solved by the Patterson method and subsequent difference Fourier techniques. SHELXS-97[1] and SHELXL-97[2] were used for the structure solution and refinement. All non-hydrogen atoms were refined anisotropically. Hydrogen atoms were placed at calculated positions and refined as riding atoms with isotropic displacement parameters.

Table S1 Crystallographic data of $Q_{p\text{-NO}}$.MeCN, **1**.EtOH and **2**

Formula	$C_{27}H_{25}N_3O$.MeCN	$C_{27}H_{25}Cl_2N_3OPd.C_2H_6O$	$C_{27}H_{27}N_2PRhCl_3$
CCDC Number	979387	979388	979389
Fw	448.55	630.87	619.74
crystal colour	dark red	dark green	yellowish brown
crystal system	triclinic	triclinic	monoclinic
space group	*P*-1	*P*-1	*P*2(1)/*c*
a, Å	9.4903(8)	10.792(2)	15.9397(5)
b, Å	10.9524(10)	11.159(2)	9.5342(3)
c, Å	13.6734(12)	12.170(2)	19.3761(6)
α° β° γ°	70.137(5) 70.544(5) 77.237(4)	100.53(2) 90.62(2) 104.71(2)	90.00 113.7200(10) 90.00
V, Å^3	1251.02(19)	1391.2(4)	2695.87(15)
Z	2	2	4
T, K	296(2)	100(2)	293(2)
calcd, g cm^{-3}	1.191	1.506	1.527
unique reflections	4296	9549	3730
refection (I>2σ(I))	3107	8583	3097
λ, Å /μ, mm^{-1}	0.71073/0.074	0.71073/0.890	0.71073/1.009
F(000)	476	644	1256
R1[a][I>2σ(I))]/GoF[b]	0.0507 / 0.849	0.0494 / 1.058	0.0399 /1.035
R1[a] (all data)	0.0685	0.0547	0.0484
wR2[c] (I>2σ (I))	0.1826	0.1257	0.1263
No. of parameters / restr.	319 / 0	347 / 3	312/1
residual density, *eÅ^{-3}*	0.224	2.253	1.012

Observation criterion: [a]$R1 = \Sigma||F_o|-|F_c||/\Sigma|F_o|$. [b]$GooF = \{\Sigma[w(F_o^2-F_c^2)^2]/(n-p)\}^{1/2}$,
[c]$wR2 = [\Sigma[w(F_o^2-F_c^2)^2]/\Sigma[w(F_o^2)^2]]^{1/2}$ where $w = 1/[\sigma^2(F_o^2)+(aP)^2+bP]$, $P = (F_o^2+2F_c^2)/3$.

Table S2 Selected experimental and calculated bond lengths (Å) of $Q_{p\text{-NO}}$.MeCN and $Q_{p\text{-NO}}$

	Bond lengths (Å)	
	experimental	**calculated**
C(2)-N(1)	1.336(2)	1.362
C(7)-N(8)	1.287(2)	1.301
C(9)-N(8)	1.413(2)	1.399
C(15)- N(1)	1.411(2)	1.404
C(5)-N(21)	1.346(2)	1.373
C(4)-O(29)	1.236(2)	1.232
C(2)-C(7)	1.499 (2)	1.505
C(2)-C(3)	1.364(2)	1.369
C(3)-C(4)	1.408(2)	1.446
C(4)-C(5)	1.499(2)	1.517
C(5)-C(6)	1.348(2)	1.369
C(6)-C(7)	1.419(2)	1.439

Table S3 Selected experimental and calculated bond lengths (Å) and angles (deg) of **1**.EtOH and **1**

	Bond parameters (Å)	
	experimental (1.EtOH)	**calculated (1)**
Pd(1)-N(1)	2.010(18)	2.081
Pd(1)-N(8)	2.017(19)	2.079
Pd(1)-Cl(1)	2.278(7)	2.321
Pd(1)-Cl(2)	2.286(1)	2.325
C(2)-N(1)	1.309(3)	1.315
C(7)-N(8)	1.322(2)	1.322
C(5)-N(21)	1.350(3)	1.369
C(4)-O(29)	1.321(2)	1.363
C(2)-C(7)	1.481(3)	1.482
C(2)-C(3)	1.431(3)	1.441
C(3)-C(4)	1.364(3)	1.358
C(4)-C(5)	1.479(3)	1.469
C(5)-C(6)	1.374(3)	1.377
C(6)-C(7)	1.409(3)	1.431
C(9)-N(8)	1.430(3)	1.424
C(15)-N(1)	1.433(3)	1.424
N(1)-Pd(1)-N(8)	80.49(8)	78.81
N(1)-Pd(1)-Cl(2)	95.85(6)	95.62
N(8)-Pd(1)-Cl(1)	94.01(5)	95.56
Cl(1)-Pd(1)-Cl(2)	89.69(3)	90.00

Table S4 Selected experimental and calculated bond lengths (Å) and angles (deg) of **2** and $\mathbf{2^{Me}}$ (PMe_3 analogue of **2**)

	Bond parameters (Å)	
	experimental	**calculated**
Rh-N(10)	2.017(4)	2.041
Rh-N(20)	2.162(4)	2.230
Rh-Cl(1)	2.3973(12)	2.421
Rh-Cl(2)	2.3141(11)	2.371
Rh-Cl(3)	2.3710(11)	2.419
Rh-P(30)	2.3070(13)	2.337
Cl(2)-Rh-Cl(1)	94.15(4)	91.95
Cl(3)-Rh-Cl(1)	170.70(4)	174.05
N(10)-Rh-Cl(1)	85.75(10)	88.00
N(10)-Rh-N(20)	90.09(18)	92.41
N(10)-Rh-P(30)	96.54(14)	96.16
N(10)-Rh-Cl(3)	86.08(11)	87.94

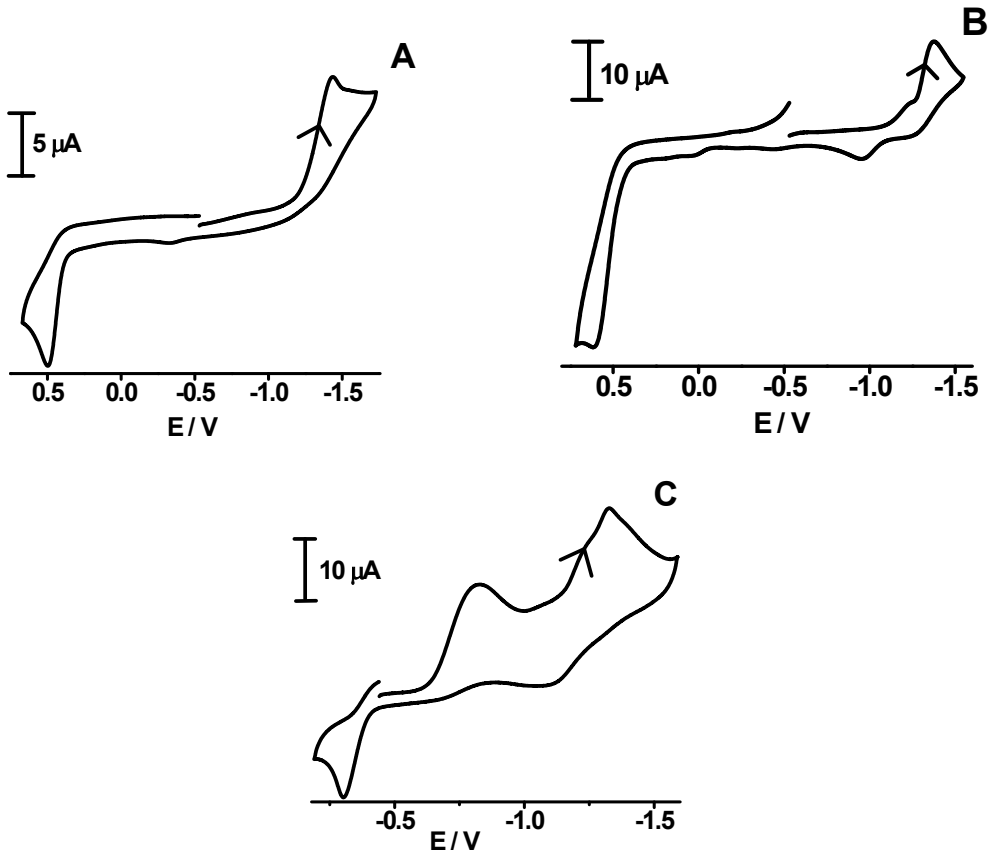

Fig. S2 Cyclic voltammograms of (A) $Q_{p\text{-NO}}$ in CH_3CN, (B) $Q_{p\text{-NO}}$ in DMSO and (C) **1** in DMF using 0.20 M $[N(n\text{-}Bu)_4]PF_6$ at 298 K.

Density functional theory (DFT) calculations

All calculations reported in this article were done with the Gaussian 03W[3] program package supported by GaussView 4.1. The DFT[4] and TD DFT[5] calculations were performed at the level of Becke three parameter hybrid functional with the non-local correlation functional of Lee-Yang-Parr (B3LYP)[6].

Gas-phase geometries $Q_{p\text{-NO}}$, $Q_{o\text{-NN}}$, $Q_{p\text{-NN}}$, $Q_{o\text{-NO}}$, **1**, $\mathbf{2^{Me}}$ (PMe_3 analogue of **2**), $[(Q_{p\text{-NO}})ZnCl_2]^-$ and $(Q_{o\text{-NN}})ZnCl_2$ with singlet spin state were optimized using Pualy's Direct Inversion[7] in the Iterative Subspace (DIIS), 'tight' convergent SCF procedure[8] ignoring symmetry with the converging criteria. In all calculation, a LANL2DZ basis set along with the corresponding effective core potential (ECP) was used for palladium and zinc metals[9-11]. Valence double zeta basis set, 6-31G[12] for H was used. For C, O, N and Cl non-hydrogen atoms valence double zeta plus diffuse and polarization functions, 6-31++G**[13] as basis set were employed for the calculations. The sixty lowest singlet excitation energies on the optimized geometries of $Q_{p\text{-NO}}$ and **1** were calculated by the TD DFT method.

Table S5 Gas phase optimized coordinates of $Q_{p\text{-NO}}$ at the B3LYP level of the theory

Sl	Sym	X	Y	Z	Sl	Sym	X	Y	Z
1	C	-0.97412	-1.42751	-0.58496	29	H	-0.74989	5.386646	1.997935
2	C	0.432076	-1.56872	-0.28019	30	H	2.348605	6.209089	-0.85888
3	C	1.251828	-0.5019	-0.0295	31	C	3.464379	-1.61389	0.428245
4	C	0.68671	0.892552	-0.05088	32	C	3.073988	-2.83444	1.000141
5	C	-0.72119	1.040349	-0.31071	33	C	4.816619	-1.43067	0.093957
6	C	-1.55066	-0.02474	-0.53861	34	C	4.014334	-3.84443	1.198305
7	H	0.809464	-2.58132	-0.33267	35	H	2.051562	-2.98269	1.325406
8	H	-1.1188	2.050118	-0.34475	36	C	5.74305	-2.44559	0.308477
9	O	-1.67514	-2.38331	-0.92003	37	H	5.134429	-0.48611	-0.34117
10	C	-4.01453	-0.61874	-0.71677	38	C	5.361237	-3.67987	0.853279
11	C	-5.09891	-0.39531	-1.57264	39	H	3.689142	-4.78054	1.64677
12	C	-4.15439	-1.54486	0.326254	40	H	6.783689	-2.2766	0.040809
13	C	-6.29332	-1.09404	-1.39896	41	N	1.550795	1.843954	0.149208
14	H	-5.0017	0.321884	-2.38457	42	N	2.587792	-0.53443	0.232069
15	C	-5.34514	-2.24577	0.476784	43	H	-3.06963	1.144699	-1.13796
16	H	-3.33493	-1.71503	1.014255	44	C	-7.71911	-2.82239	-0.20445
17	C	-6.43895	-2.03931	-0.37883	45	H	-8.04205	-2.8384	0.843511
18	H	-7.12176	-0.90312	-2.0772	46	H	-8.53322	-2.39582	-0.79957
19	H	-5.43187	-2.96357	1.289623	47	H	-7.59525	-3.86755	-0.51783
20	N	-2.86078	0.18491	-0.89092	48	C	0.529602	7.468013	0.753613
21	C	1.222625	3.197678	0.280039	49	H	1.298489	7.920829	1.39423
22	C	0.23219	3.674096	1.159028	50	H	0.56269	7.99413	-0.20755

23	C	1.995722	4.140898	-0.42262	51	H	-0.44176	7.672448	1.215846
24	C	0.014687	5.043695	1.303989	52	C	6.36219	-4.79534	1.042719
25	H	-0.34153	2.967279	1.751017	53	H	7.361395	-4.4047	1.26478
26	C	1.750097	5.502546	-0.2875	54	H	6.070288	-5.46059	1.862512
27	H	2.777575	3.781472	-1.0853	55	H	6.449616	-5.41346	0.138717
28	C	0.757976	5.98455	0.581057	56	H	2.982587	0.405301	0.263677

Table S6 Gas phase optimized coordinates of $Q_{p\text{-NN}}$ at the B3LYP level of the theory

Sl	Sym.	X	Y	Z	Sl	Sym.	X	Y	Z
1	C	1.694906	-2.01582	0.322641	29	C	0.075568	-6.0418	0.896906
2	C	1.210776	-2.23476	-1.02901	30	H	1.71984	-4.86261	0.163128
3	C	1.705504	-1.30314	-2.09139	31	C	-1.30768	-6.25688	0.914722
4	C	2.463772	-0.21087	-1.75503	32	H	-3.18875	-5.54676	0.131895
5	C	2.855578	0.053625	-0.39889	33	H	0.726713	-6.70979	1.456766
6	C	2.461709	-0.94099	0.630176	34	C	3.988446	2.147752	-0.6472
7	H	1.373567	-2.68406	1.111001	35	C	5.29581	2.629001	-0.44237
8	H	2.831238	0.449902	-2.53381	36	C	3.13736	2.880687	-1.49491
9	O	2.881129	-0.67993	1.875294	37	C	5.746246	3.766237	-1.1016
10	N	1.320874	-1.48513	-3.4044	38	H	5.947366	2.084541	0.234773
11	H	1.458783	-0.663	-3.97935	39	C	3.595297	4.033771	-2.1313
12	C	1.214716	-2.68504	-4.15592	40	H	2.105344	2.566977	-1.6191
13	C	0.384679	-2.68695	-5.28146	41	C	4.906972	4.492995	-1.96172
14	C	1.976787	-3.82706	-3.87432	42	H	6.766152	4.107317	-0.93642
15	C	0.307594	-3.81361	-6.09995	43	H	2.913453	4.591792	-2.76948
16	H	-0.20989	-1.80528	-5.50827	44	C	5.40749	5.728298	-2.67268
17	C	1.875388	-4.95051	-4.68785	45	H	5.903152	6.418522	-1.97936
18	H	2.651522	-3.83053	-3.02464	46	H	6.14064	5.473961	-3.44971
19	C	1.040186	-4.97098	-5.81549	47	H	4.589007	6.270432	-3.15707
20	H	-0.34394	-3.79162	-6.97059	48	C	0.926336	-6.20704	-6.67702
21	H	2.472721	-5.82814	-4.45013	49	H	1.900781	-6.68794	-6.82181
22	N	3.583228	1.024406	0.080335	50	H	0.263595	-6.9543	-6.21994
23	N	0.327933	-3.1107	-1.39841	51	H	0.518256	-5.97038	-7.66532
24	C	-0.17095	-4.11981	-0.57426	52	C	-1.91961	-7.37492	1.725623
25	C	-1.55895	-4.36152	-0.59562	53	H	-1.16321	-8.10126	2.040475
26	C	0.641533	-4.99039	0.177308	54	H	-2.40512	-6.99231	2.633682
27	C	-2.11162	-5.39366	0.152349	55	H	-2.68616	-7.91325	1.155555
28	H	-2.18596	-3.71603	-1.20318	56	H	3.400434	0.158336	1.777414

Table S7 Gas phase optimized coordinates of $Q_{o\text{-}NO}$ at the B3LYP level of the theory

Sl	Sym	X	Y	Z	Sl	Sym	X	Y	Z
1	C	2.165682	-1.59282	-0.29978	29	C	3.017573	-5.90338	0.526665
2	C	1.185822	-2.12649	-1.10005	30	H	3.32817	-4.03169	-0.48244
3	C	0.485069	-1.25527	-2.06223	31	C	2.113735	-6.88555	0.950728
4	C	0.780069	0.064307	-2.11196	32	H	0.024933	-7.42198	0.982261
5	C	1.789193	0.712648	-1.27802	33	H	4.081513	-6.04651	0.70139
6	C	2.52944	-0.19295	-0.30123	34	C	2.713199	3.018675	-1.07454
7	H	2.669853	-2.19252	0.446593	35	C	2.48497	4.233801	-1.76964
8	H	0.274418	0.715188	-2.81916	36	C	3.683365	3.027733	-0.0428
9	O	3.387545	0.228363	0.48649	37	C	3.186469	5.390284	-1.46533
10	N	-0.55064	-1.83231	-2.84947	38	H	1.740482	4.2232	-2.55946
11	H	-1.33344	-1.20086	-2.97769	39	C	4.374457	4.197748	0.253288
12	C	-0.27371	-2.58735	-4.02399	40	H	3.874842	2.113798	0.500771
13	C	-1.3518	-3.02353	-4.8103	41	C	4.146556	5.395827	-0.44076
14	C	1.025764	-2.93443	-4.41066	42	H	2.991688	6.303023	-2.02396
15	C	-1.12854	-3.78414	-5.95334	43	H	5.117403	4.180716	1.048115
16	H	-2.36742	-2.76172	-4.52024	44	C	4.889549	6.658246	-0.07855
17	C	1.230211	-3.71255	-5.55146	45	H	4.998867	7.322495	-0.9426
18	H	1.876759	-2.58579	-3.83497	46	H	4.354173	7.221699	0.69824
19	C	0.166715	-4.15399	-6.34552	47	H	5.888357	6.437853	0.313048
20	H	-1.98059	-4.10094	-6.55113	48	C	0.397261	-5.01052	-7.56909
21	H	2.249015	-3.9683	-5.83396	49	H	1.435275	-4.94551	-7.9117
22	N	1.914373	1.984274	-1.53199	50	H	0.186315	-6.06924	-7.36591
23	N	0.737729	-3.42236	-1.07248	51	H	-0.24979	-4.70789	-8.40065
24	C	1.230348	-4.53944	-0.37362	52	C	2.582542	-8.11647	1.690466
25	C	0.315291	-5.52304	0.033986	53	H	3.612074	-8.37702	1.422292
26	C	2.596147	-4.74926	-0.1313	54	H	2.559306	-7.96354	2.778083
27	C	0.754847	-6.67492	0.678715	55	H	1.947718	-8.98232	1.47231
28	H	-0.74593	-5.37744	-0.15495	56	H	-0.14173	-3.5532	-1.55972

Table S8 Gas phase optimized coordinates of $Q_{o\text{-}NN}$ at the B3LYP level of the theory

Sl	Sym.	X	Y	Z	Sl	Sym.	X	Y	Z
1	C	-0.37949	-1.42511	-0.8421	29	H	-0.11303	6.213328	2.263765
2	C	0.943507	-1.275	-0.58082	30	H	-1.48683	5.59203	-1.75692
3	C	1.52666	0.007036	-0.21564	31	C	3.746994	-0.78228	0.028513
4	C	0.585653	1.185956	-0.1358	32	C	3.646917	-1.88724	0.896672
5	C	-0.82379	0.926334	-0.3679	33	C	4.932335	-0.63518	-0.7204
6	C	-1.32061	-0.30977	-0.66469	34	C	4.685476	-2.81377	0.989097
7	H	1.61886	-2.11107	-0.73923	35	H	2.766818	-1.99201	1.52478
8	H	-1.5151	1.749853	-0.22314	36	C	5.944713	-1.58319	-0.64093
9	O	-0.9267	-2.57141	-1.31946	37	H	5.028401	0.230316	-1.36901

10	C	-3.50231	-1.52058	-0.39209	38	C	5.847427	-2.69029	0.218714
11	C	-4.76308	-1.72217	-0.97085	39	H	4.589252	-3.65004	1.678799
12	C	-3.1346	-2.29922	0.712586	40	H	6.840153	-1.45532	-1.24605
13	C	-5.62889	-2.6841	-0.45806	41	N	1.084349	2.325097	0.233914
14	H	-5.05793	-1.12416	-1.83	42	N	2.790647	0.229389	-0.04336
15	C	-4.00347	-3.2731	1.200737	43	H	-3.16814	0.355753	-1.13442
16	H	-2.18053	-2.13024	1.201695	44	C	-6.19064	-4.56044	1.156753
17	C	-5.26469	-3.48849	0.630552	45	H	-6.01646	-4.75339	2.220939
18	H	-6.60456	-2.81729	-0.92026	46	H	-7.24228	-4.27891	1.033711
19	H	-3.69873	-3.86542	2.06092	47	H	-6.0465	-5.51205	0.626845
20	N	-2.67406	-0.50267	-0.92357	48	C	-1.56151	7.423693	0.282693
21	C	0.368667	3.520222	0.223386	49	H	-0.81865	8.232274	0.301172
22	C	0.459297	4.361947	1.351117	50	H	-2.19134	7.57642	-0.59988
23	C	-0.34394	3.991929	-0.89692	51	H	-2.19293	7.550201	1.170851
24	C	-0.18301	5.593355	1.372087	52	C	6.975536	-3.68925	0.328839
25	H	1.033329	4.017534	2.206026	53	H	7.840019	-3.26385	0.856131
26	C	-0.95641	5.244666	-0.87249	54	H	6.664852	-4.58395	0.87848
27	H	-0.37947	3.38622	-1.79794	55	H	7.329334	-4.00814	-0.65912
28	C	-0.9013	6.06492	0.26026	56	H	-0.22427	-3.23485	-1.42136

Table S9 Gas phase optimized coordinates of **1** at the B3LYP level of the theory

Sl	Sym	X	Y	Z	Sl	Sym	X	Y	Z
1	Pd	2.015654	1.573266	-0.07989	31	H	6.227163	-1.817	-1.74845
2	Cl	1.619099	3.860421	-0.08906	32	C	4.320283	-1.16011	-1.01648
3	Cl	4.305691	1.970573	0.00591	33	H	4.106917	-0.53925	-1.88372
4	N	2.168099	-0.50212	-0.06589	34	N	-2.79056	-2.98382	-0.15851
5	C	1.012398	-1.12912	-0.07182	35	H	-2.68735	-3.97946	-0.3311
6	C	0.845997	-2.55976	-0.11254	36	C	-4.1206	-2.50687	-0.08348
7	H	1.729538	-3.19375	-0.14793	37	C	-4.50517	-1.46429	0.772674
8	C	-0.39799	-3.10291	-0.13656	38	H	-3.77212	-0.97498	1.410096
9	C	-1.61572	-2.28178	-0.11744	39	C	-5.84323	-1.07543	0.836654
10	C	-1.48935	-0.91025	-0.1013	40	H	-6.12199	-0.26392	1.510618
11	H	-2.36802	-0.27836	-0.15225	41	C	-6.83504	-1.70958	0.07374
12	C	-0.20399	-0.28275	-0.08083	42	C	-6.43733	-2.76548	-0.75947
13	N	0.011014	1.02119	-0.10087	43	H	-7.18313	-3.28766	-1.36062
14	C	-1.07975	1.933187	-0.02318	44	C	-5.10209	-3.15695	-0.84664
15	C	-1.83665	2.03832	1.150637	45	H	-4.81505	-3.97056	-1.51474
16	H	-1.58216	1.421487	2.012733	46	C	7.152231	-3.35591	0.317507
17	C	-2.88194	2.960502	1.225354	47	H	7.136888	-4.11296	1.113588
18	H	-3.45115	3.046345	2.152552	48	H	7.966463	-2.65046	0.547711
19	C	-3.20194	3.786287	0.1385	49	H	7.415139	-3.85776	-0.62509
20	C	-2.4306	3.666568	-1.02847	50	O	-0.63632	-4.44313	-0.20644
21	H	-2.64833	4.307449	-1.88437	51	H	0.199472	-4.94093	-0.25243
22	C	-1.36876	2.768156	-1.10948	52	C	-8.2754	-1.25699	0.134402

23	H	-0.75153	2.714284	-2.00391	53	H	-8.5481	-0.91712	1.143504
24	C	3.388359	-1.23072	0.026945	54	H	-8.96329	-2.06551	-0.14874
25	C	3.684666	-1.98245	1.171609	55	H	-8.45682	-0.41523	-0.55325
26	H	2.981999	-1.99769	2.004939	56	C	-4.31352	4.806215	0.230429
27	C	4.895339	-2.67213	1.257726	57	H	-3.90815	5.820571	0.373502
28	H	5.121951	-3.23881	2.162234	58	H	-4.98306	4.596507	1.076024
29	C	5.827828	-2.63605	0.211284	59	H	-4.91989	4.8257	-0.68701
30	C	5.512611	-1.87466	-0.92593					

Table S10 Gas phase optimized coordinates of $\mathbf{2^{Me}}$ (PMe_3 analogue of **2**) at the B3LYP level of the theory

Sl.	Sym	X	Y	Z
1	Rh	5.814491	12.21223	0.460595
2	Cl	6.252325	9.865728	0.065408
3	Cl	6.607004	12.80093	-1.69613
4	Cl	5.504023	14.53432	1.071138
5	N	5.251642	11.71227	2.357598
6	C	5.099429	11.44491	3.470323
7	C	4.945387	11.11271	4.88058
8	H	4.492964	10.12182	4.988979
9	H	4.311284	11.85465	5.376365
10	H	5.931587	11.11002	5.356804
11	N	7.953898	12.43262	1.05262
12	H	8.385173	11.79391	0.384833
13	H	8.12197	13.38854	0.739763
14	C	8.392082	12.2057	2.396265
15	C	8.769212	10.92148	2.806054
16	H	8.73343	10.09822	2.097438
17	C	9.166076	10.7016	4.126624
18	H	9.465835	9.699294	4.426303
19	C	9.19428	11.74289	5.06776
20	C	8.792497	13.01803	4.640227
21	H	8.797348	13.84659	5.345726
22	C	8.392875	13.25447	3.323207
23	H	8.065559	14.24442	3.016479
24	P	3.697631	12.0764	-0.47065
25	C	9.684025	11.50884	6.47969
26	H	10.77143	11.64897	6.550105
27	H	9.22202	12.20653	7.187569
28	H	9.46771	10.48907	6.818579
29	C	3.547994	10.82931	-1.80709
30	H	2.534735	10.85024	-2.22571
31	H	4.278854	11.06133	-2.58629
32	H	3.775521	9.836433	-1.41275
33	C	3.117218	13.64127	-1.23066

34	H	2.130012	13.49162	-1.68389
35	H	3.071891	14.42547	-0.47166
36	H	3.837233	13.94782	-1.99397
37	C	2.381481	11.62959	0.735269
38	H	2.344696	12.38094	1.529736
39	H	1.405912	11.58416	0.237306
40	H	2.604519	10.6541	1.177722

Table S11 Gas phase optimized coordinates of [($Q_{o\text{-}NN}$)$ZnCl_2$] at the B3LYP level of the theory

Sl	Sym	X	Y	Z	Sl	Sym	X	Y	Z
1	C	-0.70698	-1.28748	-0.7325	31	C	3.410152	-1.62719	0.441807
2	C	0.596138	-1.45099	-0.38189	32	C	2.946953	-2.69181	1.232928
3	C	1.434457	-0.33821	-0.0099	33	C	4.681615	-1.71839	-0.15345
4	C	0.814086	1.035731	-0.03801	34	C	3.732314	-3.83151	1.396604
5	C	-0.5767	1.130422	-0.3803	35	H	2.002026	-2.60183	1.760167
6	C	-1.34516	0.040051	-0.70122	36	C	5.438884	-2.87301	0.001565
7	H	1.055053	-2.43107	-0.46187	37	H	5.050437	-0.88348	-0.74334
8	H	-1.0283	2.115079	-0.40475	38	C	4.983951	-3.95045	0.779587
9	O	-1.47722	-2.28828	-1.20822	39	H	3.3698	-4.63779	2.029867
10	C	-3.77126	-0.6092	-0.84228	40	H	6.412298	-2.93327	-0.47923
11	C	-4.86219	-0.58516	-1.71972	41	N	1.600559	2.041905	0.244529
12	C	-3.85571	-1.36513	0.332583	42	N	2.69996	-0.419	0.290956
13	C	-6.01202	-1.31342	-1.42656	43	H	-2.86687	1.1423	-1.42205
14	H	-4.80205	-0.00074	-2.63441	44	C	-7.33927	-2.9156	0.024676
15	C	-5.00446	-2.10578	0.601498	45	H	-7.45081	-3.10347	1.097652
16	H	-3.03483	-1.35808	1.04328	46	H	-8.24669	-2.41238	-0.32635
17	C	-6.10371	-2.09702	-0.26758	47	H	-7.29744	-3.89301	-0.47473
18	H	-6.85109	-1.27802	-2.11736	48	C	0.188553	7.583309	0.787373
19	H	-5.05439	-2.68613	1.519826	49	H	0.965938	8.108452	1.357019
20	N	-2.63993	0.1932	-1.14912	50	H	0.113075	8.081887	-0.18651
21	C	1.179325	3.382143	0.358754	51	H	-0.76054	7.725158	1.313787
22	C	0.083047	3.776652	1.143898	52	C	5.839107	-5.18	0.970342
23	C	1.965448	4.369905	-0.26275	53	H	6.721084	-4.95711	1.584517
24	C	-0.23005	5.128391	1.275933	54	H	5.284145	-5.98189	1.467377
25	H	-0.48491	3.031192	1.691944	55	H	6.205475	-5.56539	0.0114
26	C	1.622748	5.710802	-0.13899	56	Cl	4.970813	2.025991	-1.1363
27	H	2.829997	4.067176	-0.84759	57	Cl	4.097875	1.728052	2.867143
28	C	0.522259	6.118861	0.632503	58	Zn	3.665349	1.505769	0.659519
29	H	-1.06831	5.418133	1.905124	59	H	-0.94982	-3.10307	-1.26407
30	H	2.232801	6.459134	-0.63928					

Table S12 Gas phase optimized coordinates of $[(Q_{o\text{-}NO})ZnCl_2]^-$ at the B3LYP level of the theory

Sl	Sym	X	Y	Z	Sl	Sym	X	Y	Z
1	C	-0.67718	-2.40269	-1.37747	30	H	1.393389	5.927485	0.06786
2	C	0.408211	-1.85654	-0.70742	31	C	2.607534	-0.51407	0.782387
3	C	0.610065	-0.45576	-0.52301	32	C	2.993399	-0.12624	2.083238
4	C	-0.39742	0.467427	-1.14129	33	C	3.4335	-1.44176	0.110573
5	C	-1.46002	-0.03505	-1.84006	34	C	4.116311	-0.67256	2.694436
6	C	-1.65945	-1.44777	-2.018	35	C	4.570096	-1.96171	0.725582
7	H	1.093021	-2.54893	-0.23418	36	H	3.189703	-1.73135	-0.90681
8	H	-2.18592	0.646176	-2.27307	37	C	4.92986	-1.60397	2.031592
9	O	-0.89445	-3.6603	-1.48608	38	H	4.376849	-0.36052	3.704803
10	C	-3.61864	-1.29397	-3.39516	39	H	5.191232	-2.66691	0.175528
11	C	-3.29416	-0.35393	-4.386	40	N	-0.3452	1.835336	-0.9118
12	C	-4.9715	-1.61064	-3.1792	41	N	1.524046	0.136915	0.206043
13	C	-4.30276	0.274442	-5.11704	42	C	-6.7462	0.686656	-5.66755
14	H	-2.2509	-0.14719	-4.60478	43	H	-7.30287	1.397838	-5.0415
15	C	-5.96453	-0.96372	-3.9073	44	H	-6.3369	1.246491	-6.5156
16	H	-5.21897	-2.37058	-2.44286	45	H	-7.47635	-0.03083	-6.06187
17	C	-5.65381	-0.0074	-4.88652	46	C	3.889693	5.73194	-1.06283
18	H	-4.02956	0.989696	-5.89062	47	H	4.331845	5.819438	-2.06325
19	H	-7.00581	-1.21955	-3.72091	48	H	3.521791	6.722487	-0.77299
20	N	-2.64007	-2.00905	-2.67423	49	H	4.705919	5.471805	-0.37476
21	C	0.742027	2.734315	-0.92996	50	C	6.137265	-2.21138	2.707802
22	C	1.954114	2.474034	-1.58933	51	H	6.892835	-2.52149	1.976702
23	C	0.558845	3.992695	-0.34246	52	H	6.610237	-1.50396	3.39964
24	C	2.951706	3.440828	-1.62389	53	H	5.87021	-3.10315	3.292966
25	H	2.109885	1.515177	-2.06911	54	Zn	-2.5735	-4.1974	-2.50319
26	C	1.56371	4.959025	-0.39857	55	Cl	-4.3769	-4.81589	-1.1983
27	H	-0.37532	4.208546	0.171591	56	Cl	-2.16681	-5.20363	-4.52373
28	C	2.783722	4.702446	-1.03028	57	H	-1.23541	2.291337	-1.06709
29	H	3.884161	3.212794	-2.13679	58	H	2.384182	0.612114	2.596518

Table S13 Excitation energies (λ/nm), oscillator strengths (f) and dominant contributions of UV-Vis/NIR absorption bands of $Q_{p\text{-NO}}$ obtained from the TD DFT calculations

λ_{cal} (nm)	f	λ_{exp} (nm)	Significant transition	Percentage (>10%)
605	0.1475	544	HOMO→LUMO	82.35
475	0.2980		HOMO-2 → LUMO HOMO-1 → LUMO	25.62 59.67
459	0.2268	-	HOMO-2 → LUMO HOMO-1 → LUMO	59.06 23.27
394	0.0758	392	HOMO-7→ LUMO HOMO-3 →LUMO	16.61 58.59

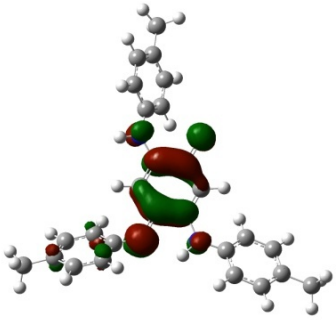

LUMO

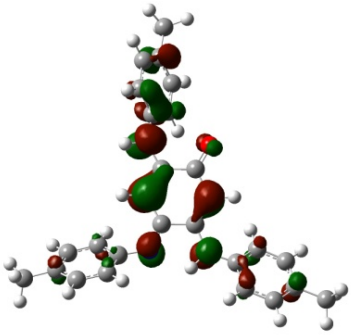

HOMO

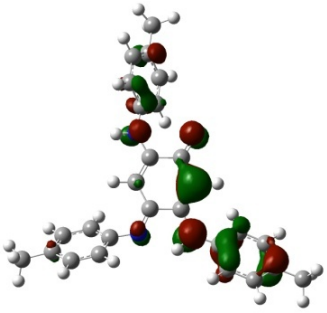

HOMO-1

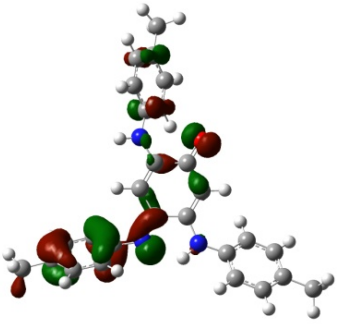

HOMO-2

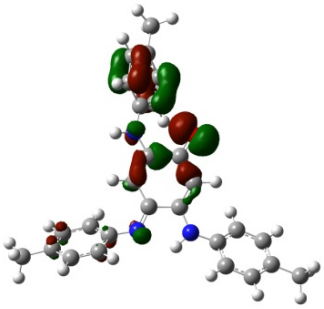

HOMO-3

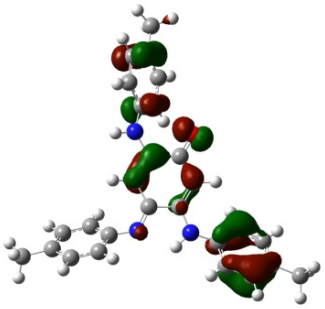

HOMO-7

Fig. S3 Photo active molecular orbitals of $Q_{p\text{-NO}}$ (isosurface value, 0.04).

Table S14 Excitation energies (λ/nm), oscillator strengths (f), transition types and dominant contributions of UV-Vis/NIR absorption bands of **1** obtained from the TD DFT calculations

λ_{cal} (nm)	f	λ_{exp} (nm)	Significant transition	Percentage (>10%)	Transition types
609	0.1383	671	HOMO-4 → LUMO HOMO-3 → LUMO HOMO-2 → LUMO	10.20 38.14 23.89	MLCT MLCT MLCT
579	0.1026	617	HOMO-4 → LUMO HOMO-6 → LUMO	61.39 40.11	MLCT MMLLCT
522	0.0928	452	HOMO → LUMO+1	31.78	d-d
MLCT = Metal to ligand charge transfer MMLLCT = Mixed metal ligand to ligand charge transfer					

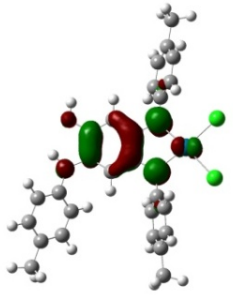

LUMO

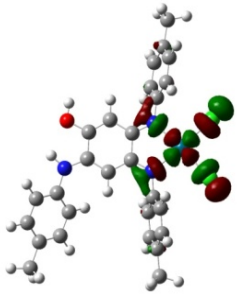

LUMO+1

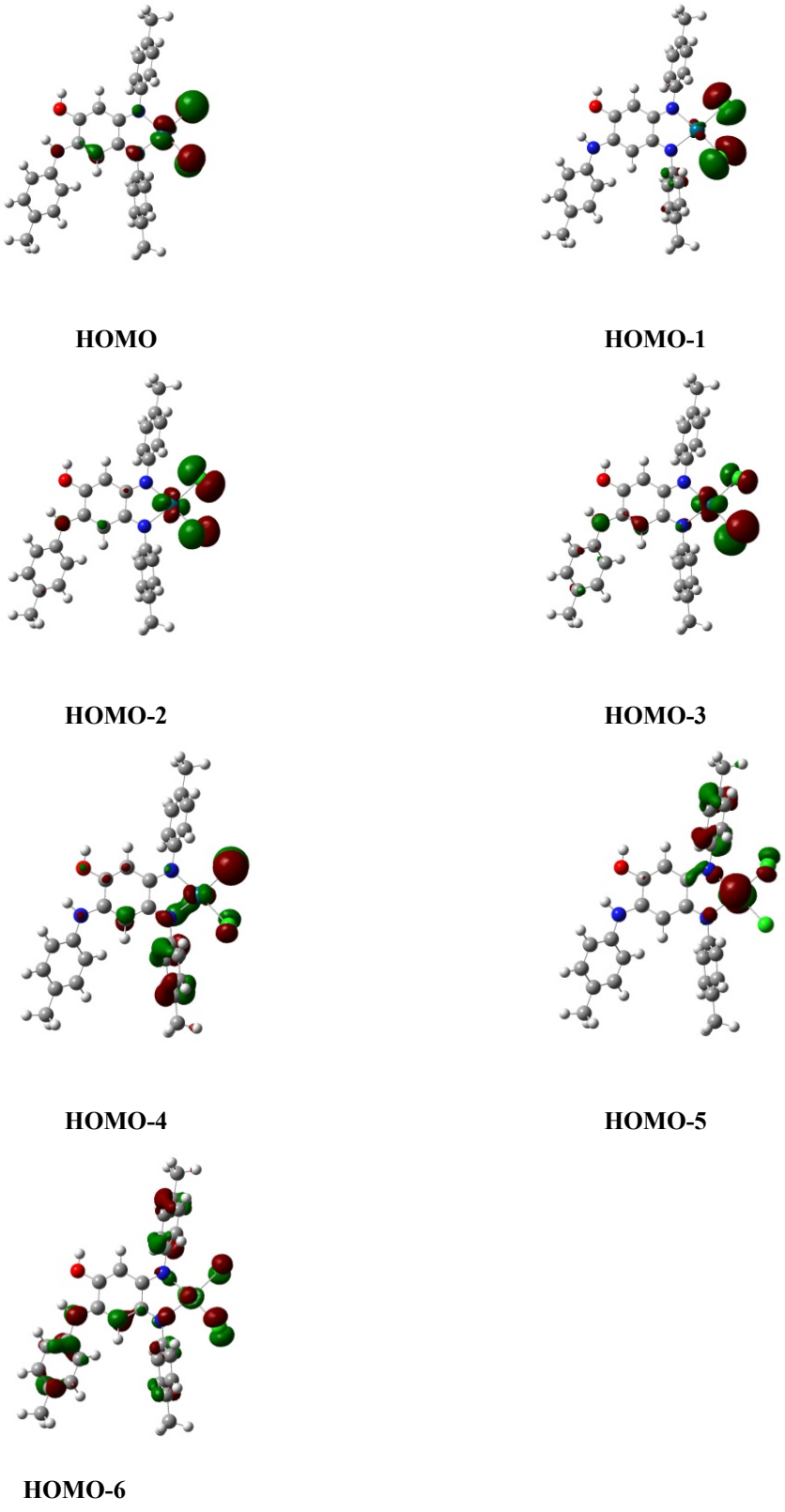

Fig. S4 Photo active molecular orbitals of **1** (isosurface value, 0.04).

References

1 ShelXS97, G. M. Sheldrick, Universität Göttingen: Germany, 1997.

2 ShelXL97, G. M. Sheldrick, Universität Göttingen: Germany, 1997.

3 M. J. Frisch, G. W. Trucks, H. B. Schlegel, G. E. Scuseria, M. A. Robb, J. R. Cheeseman, Jr., J. A. Montgomery, T. Vreven, K. N. Kudin, J. C. Burant, J. M. Millam, S. S. Iyengar, J. Tomasi, V. Barone, B. Mennucci, M. Cossi, G. Scalmani, N. Rega, G. A. Petersson, H. Nakatsuji, M. Hada, M. Ehara, K. Toyota, R. Fukuda, J. Hasegawa, M. Ishida, T. Nakajima, Y. Honda, O. Kitao, H. Nakai, M. Klene, X. Li, J. E. Knox, H. P. Hratchian, J. B. Cross, R. Ammi, C. Pomelli, J. W. Ochterski, P. Y. Ayala, K. Morokuma, G. A. Voth, P. Salvador, J. J. Dannenberg, V. G. Zakrzewski, S. Dapprich, A. D. Daniels, M. C. Strain, O. Farkas, D. K. Malick, A. D. Rabuck, K. Raghavachari, J. B. Foresman, J. V. Ortiz, Q. Cui, A. G. Baboul, S. Clifford, J. Cioslowski, B. B. Stefanov, G. Liu, A. Liashenko, P. Piskorz, I. Komaromi, R. L. Martin, D. J. Fox, T. Keith, M. A. Al-Laham, C. Y. Peng, A. Nanayakkara, M. Challacombe, P. M. W. Gill, B. Johnson, W. Chen, M. W. Wong, C. Gonzalez and J. A. Pople, Gaussian 03, revision E.01; Gaussian, Inc.: Wallingford, CT 06492, 2005.

4 (a) D. R Salahub and M. C. Zerner, *The Challenge of d and f Electrons,* ACS, Washington, D.C., 1989; (b) R. G. Parr and W. Yang, *Density Functional Theory of atoms and molecules*; Oxford University Press, Oxford, U.K., 1989; (c) W. Kohn and L. Sham, *J. Phys. Rev*., 1965, **140**, A1133; (d) P. Hohenberg and W. Kohn, *Phys Rev*., 1964**, 136***,* B864.

5 (*a*) R. E. Stratmann, G. E. Scuseria and M. Frisch, *J. Chem. Phys*., 1998, **109**, 8218; (*b*) M. E. Casida, C. Jamoroski, K. C. Casida and D. R. Salahub, *J. Chem. Phys*., 1998, **108**, 4439; (*c*) R. Bauernschmitt and R. Ahlrichs, *Chem. Phys.Lett*., 1996, **256**, 454.

6 (*a*) A. D. Becke, *J. Chem. Phys*.**,** 1993, **98**, 5648; (*b*) B. Miehlich, A. Savin, H. Stoll, H. Preuss, *Chem. Phys. Lett.*, 1989, **157**, 200; (*c*) C. Lee, W. Yang, R. G. Parr, *Phys. Rev*., 1988, **B 37**, 785.

7 P. J. Pulay, *Comp. Chem*.,1982, **3**, 556.

8 H. B. Schlegel and J. J. McDouall, in *Computational Advances in Organic Chemistry,* ed. C. Ogretir and I. G. Csizmadia, Kluwer Academic, The Netherlands, 1991, p 167.

9 P. J. Hay and W. R. Wadt, *J. Chem. Phys*.,1985, **82**, 270.

10 W. R. Wadt and P. J. Hay, *J. Chem. Phys*.,1985, **82**, 284.

11 P. J. Hay and W. R. Wadt, *J. Chem. Phys*.,1985, **82**, 299.

12 (*a*) V. A. Rassolov, M. A. Ratner, J. A. Pople, P. C. Redfern and L. A. Curtiss, *J. Comp. Chem.,* 2001, **22**, 976; (b) M. M. Francl, W. J. Pietro, W. J. Hehre, J. S. Binkley, D. J. DeFrees, J. A. Pople and M. S. Gordon, *J. Chem. Phys.*, 1982, **77**, 3654; (*c*) P. C. Hariharan and J. A. Pople, *Mol. Phys.,* 1974**, 27**, 209; (d) P. C. Hariharan and J. A. Pople, *Theo. Chim. Acta.,* 1973**, 28**, 213; (*e*) W. J. Hehre, R. Ditchfield and J. A. Pople, *J. Chem. Phy.,* 1972, **56**, 2257.

13 T. Clark, J. Chandrasekhar, G. W. Spitznagel and P. V. R. Schleyer, *J. Comp. Chem.,* 1983, **4**, 294.